SCEC 2003 Research Annual Report of Research

by Andrew Meigs[1] and Michele Cooke[2]

[1]Department of Geosciences, Oregon State University, Corvallis, OR, 97331
[2] Geosciences Department, University of Massachusetts, Amherst, MA, 01003

Constraining Blind Thrust Fault Topology with Elastic Models of Topography and Deformed Geologic Markers

The representation of fault surfaces in three-dimensions is imperative for understanding how regional fault networks accommodate strain, interact, and are organized internally. Our work over the last year sought to evaluate proposed configurations of the Puente Hills Thrust (PHT) system in the Los Angeles basin using geologic data and three-dimensional mechanical models. Structural cross-sections, three-dimensional mechanical modeling, and topographic analysis were combined to evaluate permissible fault models for blind thrust faults in the northern Los Angeles basin (LAb). The integrated geologic and modeling evaluative approach we employed for this relatively well-studied region of Southern California serves as a basis for validation of portions of the community fault model (CFM), explored the compatibility between geodetic models for the direction and rate of horizontal contraction, and identified areas where the CFM and geologic data are not in good agreement.

<u>Methods</u>

Rock uplift was measured relative to the undeformed axis of the LAb for the base of the Pico Member of the Fernando Formation (~2.9 Ma) and for the base of Quaternary units (~1.4 Ma) on 8 cross-sections across the northern LAb from the Elysian Hills west of downtown LA to the Coyote Hills on the east (Figs. 1 and 2). Each cross-section was constrained by numerous wells. Well control typically extended to ~3 km depth, which constrained tightly the structural geometry of the Pico Member and the base of the Quaternary sediments. Rock uplift rate was calculated from the structural relief of each stratigraphic marker divided by the marker age. Individual measurements of structural relief (or rate) measured along each section were assigned a UTM northing and easting coordinate. Maps of rock uplift and uplift rate were generated by contouring the spatial values of relief and rate (Fig. 4). These maps serve to constrain the spatial pattern of rock uplift and rock uplift rate in two time slices (2.9 and 1.4 Ma, respectively).

The deformation of the northern LAb is simulated using three-dimensional Boundary Element Method (BEM) models containing fault surfaces defined by the SCEC Community Fault Model working group (Fig. 3). Within the BEM models, fault surfaces are composed of triangular elements that permit simulation of non-planar surfaces and irregular fault intersections such as are observed in the subsurface. The faults are weak in shear and slip in response to a combination of tectonic loading (determined from geodesy) and interaction with nearby faults.

An array of models simulate deformation under variations in fault intersection, tectonic loading and linkage between faults in order to assess the sensitivity of uplift pattern and magnitude to these variations. Three kinematically viable intersections between the primarily strike-slip Whittier fault and primarily reverse slip Coyote Hills segment of the PHT are simulated (Griffith and Cooke, in press). Uncertainty in the tectonic loading has arisen from the wide range in contraction directions and magnitudes determined from different geodetic studies, from 56 mstrain/yr at N36E (Bawden et al, 2001) to 100 mstrain/yr north-south (Argus, in press). Furthermore, the subsurface seismic data has left uncertainty in whether the echelon segments of the PHT are directly linked at depth or remain discrete fault surfaces (Shaw et al, 2003). Each of these variations is explored with the numerical models and the resultant uplift compared to geologic observations.

Uplift Pattern and History

Maps of rock uplift rate reveal the location and relative activity of underlying faults (Fig. 4). Uplift at the crest of the Coyote Hills, Santa Fe Springs, Montebello Hills (Elysian Park anticlinorium) and in the Elysian Hills (Las Cienegas/Santa Monica Mountains anticlinorium) is evident by 2.9 Ma (Fig. 4a). Coyote and Santa Fe Springs appear as discrete uplifts at 2.9 Ma, but define a continuous region of uplift by 1.4 Ma (Fig. 4b). Contours between Santa Fe Springs and the Montebello Hills trend north as revealed by the maps of the 2.9 and 1.4 Ma horizons (Figs. 3a and b). The Elysian Hills are characterized by an east-trend and are separated from the Montebello Hills by northwest-trending, west-sloping contours. These observations suggest that the Coyote-Santa Fe Springs structures potentially represented discrete faults at 2.9 Ma, but linked by 1.4 Ma and are now underlain by a single fault plane. Discontinuities between Coyote/Santa Fe Springs and Montebello Hills as well as Montebello Hills and Elysian Hills are suggested by the north-trend, west-slope and northwest-trend, southwest-slope of contours between them; discontinuities that may represent either tip lines or oblique ramps in the underlying faults.

Rock uplift rate between 2.9 and 1.8 Ma has decreased above the Las Cienegas/Elysian Park anticlinorium (from >1 to <0.5 mm/yr, west of downtown; ~0.6 to 0.1 mm/yr, east of downtown) remained steady above Santa Fe Springs (decrease from ~0.7 to 0.6 mm/yr), and increased nominally in the Coyote Hills (~0.6 to 0.8 mm/yr) (Fig. 4). If vertical rock uplift is a proxy for the distribution of shortening and fault slip rate, there has been a shift in the locus of deformation from the Las Cienegas/Elysian Park anticlinorium to the Puente Hills thrust system (PHT) in the southeast since ~3 Ma.

Sensitivity of uplift to fault model variations

The modeled uplift patterns are more sensitive to changes in tectonic boundary conditions than linkage of fault segments. Linking the echelon PHT fault segments below 8 km in the model does not substantially change the uplift pattern. Thus, uplift cannot be used to distinguish between hard and soft linked fault segments. However, the tectonic loading of 100 nanostrain/yr north-south contraction across the LAb produces a far better match to the observed uplift pattern and magnitude than contraction of 56 nanostrain/yr at N36E (Fig. 4c). Of the three kinematically viable fault intersections, the BEM models with the Coyote Hills extending to the base of the seismogenic crust better match the available slip rates (Griffith and Cooke, in press) and uplift patterns (Fig. 4c). The uplift pattern cannot be used to determine if the Whittier fault is active below the intersection with the Coyote Hills fault; however, mechanical efficiency analysis give preference for the Whittier slipping through the entire seismogenic crust (Griffith and Cooke, in press).

Comparison of uplift to model predictions

Modeled short-term surface uplift using the best matching intersection configuration and tectonic boundary condition is in general agreement with Quaternary deformation pattern in terms of the range in rates and in loci of high rates. The model results replicate the distinct locally high uplift rates associated with the Montebello Hills, Santa Fe Springs and Coyote Hills. In detail, the model results have less Quaternary uplift for the Coyote Hills and greater uplift above the Los Angeles fault. However, patterns of rock uplift rate based on the Pico Member (past 2.9 Ma) show good agreement with modeled rates, in general, and provide a better match in the Coyote Hills than for the Quaternary marker.

Patterns of rock uplift in the Montebello and Elysian Hills do not agree well with rates based on BEM models using the CFM. One potential explanation is that the CFM in this region is not well constrained at crustal depths, particularly if the model is based on the geometric model of the Elysian Park anticlinorium of Davis and Namson (1989). A second possible explanation is that the intersection of the Elysian Park and the Santa Monica Mountains anticlinoria is not well constrained at depth. At the surface the Hollywood fault, one element of the Santa Monica Mountains anticlinorium truncates and offsets thee Elysian Park anticlinorium (Meigs et al., 2002). How the blind structures beneath the anticlinoria and the surface faults intersect at depth is unconstrained. Thus, there is significant uncertainty in the CFM in a key locale beneath the central LA business district, which has implications for the CFM, CBM, and RELM.

References:

Argus, D. F., M. B. Heflin, G. Peltzer, F. Crampe, and F. H. Webb, Interseismic strain accumulation and anthropogenic motion in metropolitan Los Angeles, submitted to Journal of Geophyscial Research.

Bawden, G.W., Thatcher, W., Stein, R.S., Hudnut, K.W., and Peltzer, G., 2001, Tectonic contraction across Los Angeles after removal of groundwater pumping effects: Nature, v. 412, p. 812-815.

Davis, T.L., Namson, J., and Yerkes, R.F., 1989, A cross-section of the Los Angeles area: Seismically active fold and thrust belt, the 1987 Whittier Narrows earthquake, and earthquake hazard: Journal of Geophysical Research, v. 94, p. 9644-9664.

Meigs, A.J., and Oskin, M.E., 2002, Convergence, block rotation, and structural interference across the Peninsular-Transverse Ranges boundary, eastern Santa Monica Mountains, California, in Barth, A., ed., Contributions to Crustal Evolution of the Southwestern United States, Volume 365: Geological Society of America Special Paper: Boulder, Geological Society of America, p. 279-293.

Griffith and Cooke, in press, Mechanical validation of the three-dimensional intersection geometry between the Puente Hills blind-thrust system and the Whittier Fault, BSSA.

Shaw, J.H., Plesch, A., Dolan, J.F., Pratt, T.L., and Fiore, P., 2003, Puente Hills blind-thrust system, Los Angeles, California: BSSA, 92, p. 2946-2960

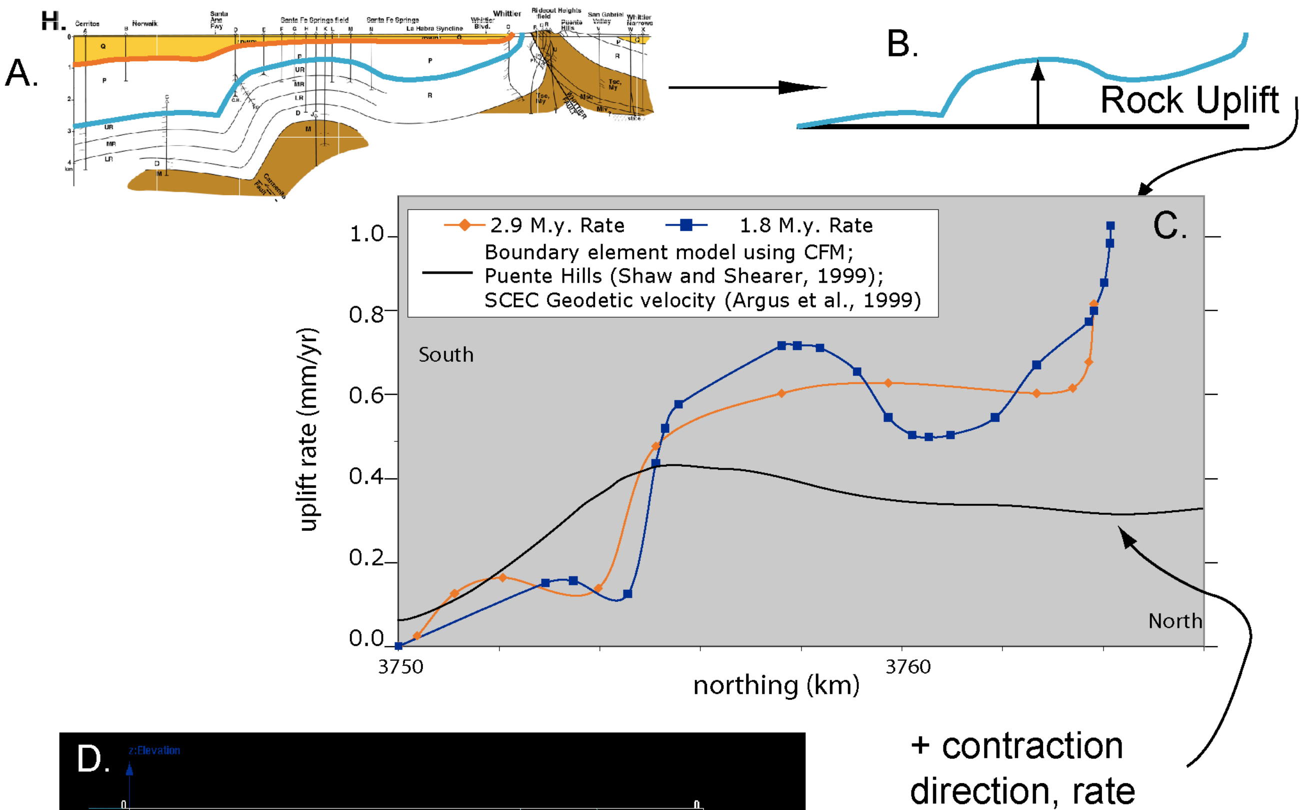

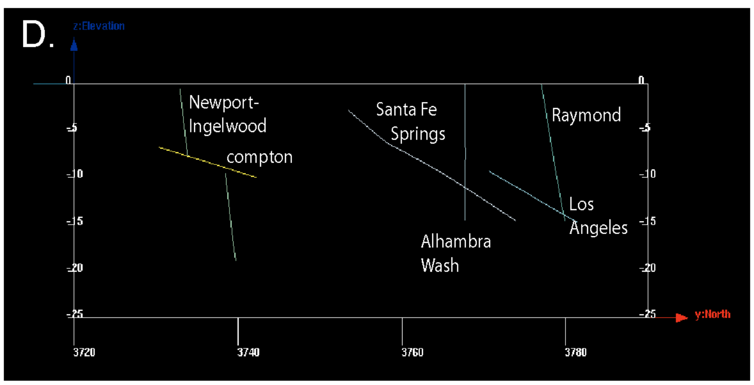

Figure 1. Deformed stratigraphic marker of a known age from a cross-section (A) is used to measure rock uplift (structural relief) relative to adjacent structural low (B). Rock uplift rate is determined along a line of section by dividing strucutral relief by age of the marker (C). Boundary element models test a range of possible intersection geometries of faults in the CFM (D). Rock uplift rate from models is derived from geodetically-constrained contraction directions and rates. Results for a line of section across the Puente Hills thrust at Santa fe Springs is shown for reference.

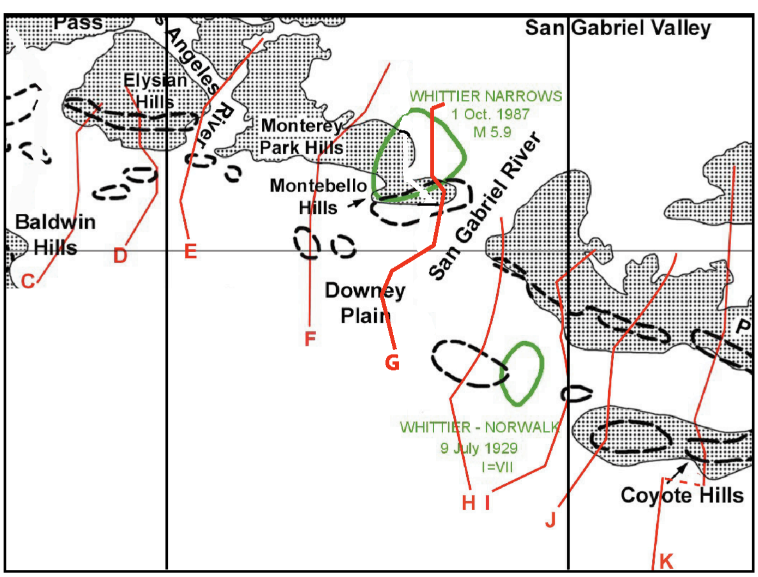

Figure 2. Location map of cross-sections used to constrain patterns of rock uplift between the Coyote Hills on the east and the Elysian Hills on the west. The approximate locations of the Whittier Narrows and Whittier-Norwalk earthquakes meizoseismal areas are illustrated for reference.

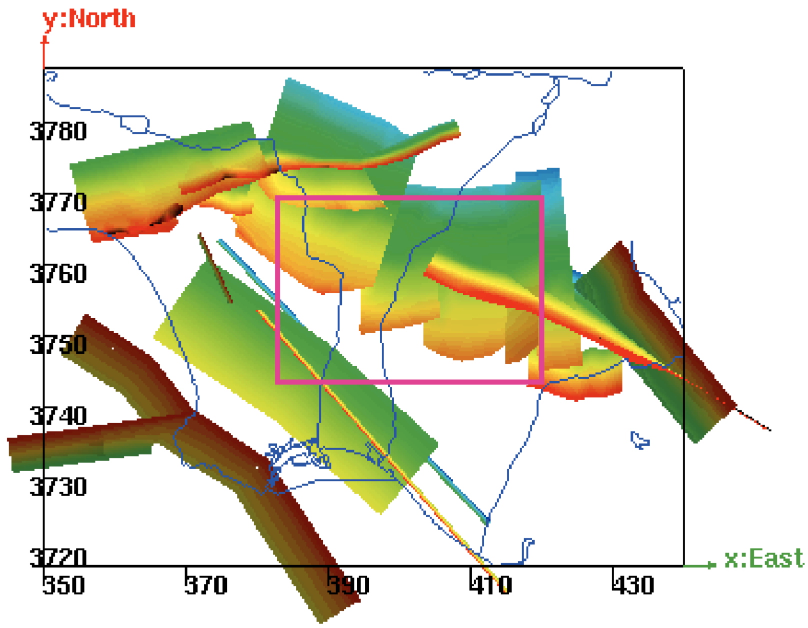

Figure 3. Map projection with northerly illumination of the fault surfaces within the BEM model. Depths along the fault surfaces range from 0km (red) to 20 km (blue). Blue lines trace rivers and the coastline wheras the magenta box outlines the area studied for uplift rates. UTM coordinate system is in kilometers (zone11 NAD 1927).

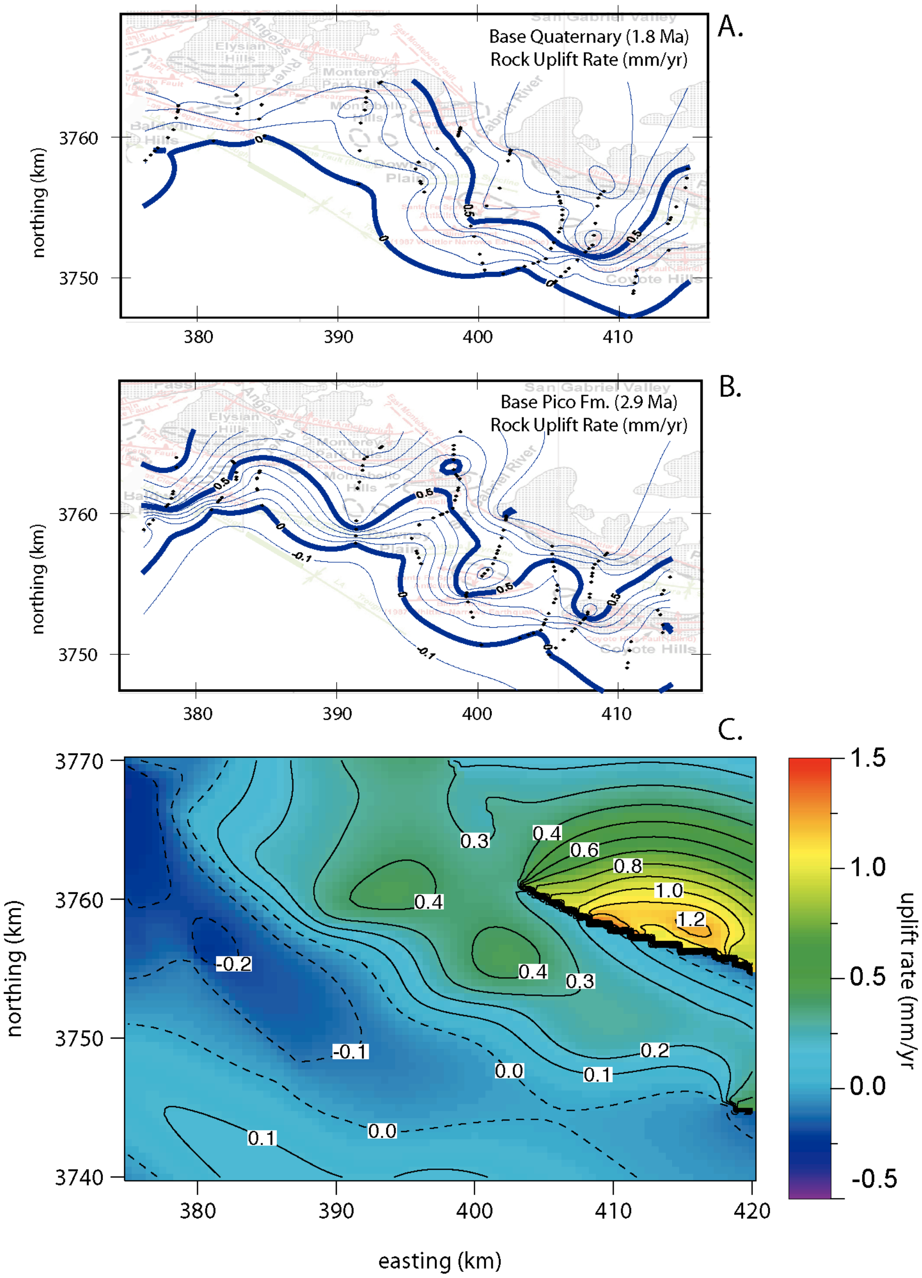

Figure 4. Maps of rock uplift rate based on the depth to the base of the Quaternary (A), depth to base of the Pico Formation (B), and a CFM-based model of faults using N-S shortening of 100 nano strain/yr. Note the decrease in rate in the northwest between Pico and Quaternary time. Rate remains steady in the southeast. The pattern of rock uplift rate in the southeast for either time slice is consistent with the pattern predicted from the model. Poor agreement between the model and observations characterizes the northwestern area. UTM coordinate system is in kilometers (zone11 NAD 1927).